Hindawi Publishing Corporation
Shock and Vibration
Volume 2015, Article ID 648097, 15 pages
http://dx.doi.org/10.1155/2015/648097

Research Article

A Bioinspired Methodology Based on an Artificial Immune System for Damage Detection in Structural Health Monitoring

Maribel Anaya,[1,2] Diego A. Tibaduiza,[2] and Francesc Pozo[3]

[1]*CoDAlab, Department of Applied Mathematics III, Universitat Politècnica de Catalunya (UPC), 08036 Barcelona, Spain*
[2]*Faculty of Electronic Engineering, Universidad Santo Tomás, Bogotá, Colombia*
[3]*CoDAlab, Department of Applied Mathematics III, Escola Universitària d'Enginyeria Tècnica Industrial de Barcelona (EUETIB), Universitat Politècnica de Catalunya (UPC), Comte d'Urgell 187, 08036 Barcelona, Spain*

Correspondence should be addressed to Francesc Pozo; francesc.pozo@upc.edu

Received 27 February 2015; Revised 5 May 2015; Accepted 14 May 2015

Academic Editor: Haifeng Gao

Among all the aspects that are linked to a structural health monitoring (SHM) system, algorithms, strategies, or methods for damage detection are currently playing an important role in improving the operational reliability of critical structures in several industrial sectors. This paper introduces a bioinspired strategy for the detection of structural changes using an artificial immune system (AIS) and a statistical data-driven modeling approach by means of a distributed piezoelectric active sensor network at different actuation phases. Damage detection and classification of structural changes using ultrasonic signals are traditionally performed using methods based on the time of flight. The approach followed in this paper is a data-based approach based on AIS, where sensor data fusion, feature extraction, and pattern recognition are evaluated. One of the key advantages of the proposed methodology is that the need to develop and validate a mathematical model is eliminated. The proposed methodology is applied, tested, and validated with data collected from two sections of an aircraft skin panel. The results show that the presented methodology is able to accurately detect damage.

1. Introduction

Structural health monitoring (SHM) is a discipline that makes use of sensors permanently attached to a structure together with different software analysis developments in order to detect damage and assess the proper performance of structures. An SHM system traditionally includes continuous monitoring, data processing algorithms, and pattern recognition techniques for a robust analysis. Different methodologies have been developed in the last years in the field of SHM. However, with the use of bioinspired algorithms, promising results have been obtained, mainly due to its adaptive, distributed, and autonomous features.

This work presents a damage detection methodology that is mainly based on an artificial immune system (AIS) as a pattern recognition technique and affinity plots to discriminate the different structural states of the structure. This methodology is applied to the collected data by a piezoelectric system. The artificial immune system has been proposed and used in several applications. However, in structural health monitoring, this methodology is relatively new. A brief state of the art in structural health monitoring is presented, in chronological order, in the next lines, highlighting the most representative works with respect to artificial immune systems.

The use of nondestructive testing inspection methods (NDT) has proved to be a very useful tool for damage detection tasks. However, in some situations where it is impossible to manually inspect a structure, as in the inspection of large-scale structures, the use of automated methods presents significant advantages. Some of these advantages can be summarized as follows: (i) continuous monitoring, since the sensors are permanently attached to the structure; (ii) early damage detection; and (iii) damage identification, among others. In this sense, structural health monitoring (SHM) extends the limits of the NDT methods by including

the use of data processing algorithms, pattern recognition, and continuous monitoring because the sensors are permanently attached to the structure. This is one of the reasons why the development of improvements in data processing algorithms is a current demand. The contribution of the present work is the development of a methodology for data-driven damage classification using a bioinspired algorithm, which is applied to data that comes from a piezoelectric system. More precisely, this work uses an artificial immune system that allows the use of this methodology as a pattern recognition approach. The use of artificial immune systems (AIS) is relatively new in the literature and, compared with the application of other approaches in SHM, there are still a reduced number of works. In the next lines we briefly compile in chronological order the most representative works in the use of AIS.

In 2003 Branco et al. [1] developed three module algorithms called T-module, B-module, and D-module. These algorithms are based on immunologic principles to detect anomalous situations in a squirrel-cage motor induction. The T-module distinguishes between self- and non-self-conditions, the B-module analyzes the occurrence of both cells (self and non-self), and finally the D-module is similar to a T-module but with a reduced space. In this work, the normal operation condition of the machine (self) is represented by the frequency spectrum that can include or not include harmonics.

In 2007, da Silva et al. [2] presented a damage detection algorithm applying an autoregressive model and autoregressive model with exogenous input (AR-ARX). This algorithm is based on the structural vibration response measurements and the residual error as damage sensitive index. Data compression is used by means of principal component analysis (PCA) and the fuzzy *c*-means clustering method is used to quantify the damage sensitive index. In this paper, the authors used a benchmark problem with several damage patterns to test the algorithm. As the main result, a structural diagnosis was obtained with high correlation with the actual state of the structure. Later, in 2008, da Silva et al. [3] developed a strategy to perform structural health monitoring. This strategy included three different phases as follows: (i) the use of principal component analysis to reduce the dimensionality of the time series data; (ii) the design of an autoregressive-moving-average (ARMA) model using data from the healthy structure under several environmental and operational conditions; and finally (iii) the identification of the state of the structure through a fuzzy clustering approach. In this paper, the authors compared the performance of two fuzzy algorithms, fuzzy *c*-means (FCM) and Gustafson-Kessel (GK) algorithms. The proposed strategy was applied to data from a benchmark structure at Los Alamos National Laboratory. The work showed that the GK algorithm outperforms the FCM algorithm, because the first algorithm considers an adaptive distance norm and allows clusters with several geometrical distributions.

Also, in 2008, Zhang et al. [4] used a clonal selection algorithm to solve a combinatorial optimization problem called *sensor optimization*. This problem consists in choosing an appropriate distribution of a set of sensors in a structure to detect impacts. To test the algorithm, the authors used a composite plate instrumented with 17 lead zirconium titanate (PZT) transducers.

Vieira de Moura et al. [5] presented a fuzzy-based metamodel to detect damage in a flat structure under corrosion conditions. This work considers data obtained from an SHM approach based on electromechanic impedance. Chen [6], in 2010, applied an agent-based artificial immune system for adaptive damage detection. In the approach, a group of agents is used as immune cells (B-cells) patrolling over a distributed sensor network installed in the structure. The damage diagnosis is based on the analysis of structural dynamic response data. Each mobile agent inspects the structure using agent-based cooperation protocols. In 2010, Tan et al. [7] presented a damage detection algorithm based on fuzzy clustering and support vector machines (SVM). In this work, as a first step, the wavelet packet transform is used to decompose the accelerator data from the structure and extract the energy of each wavelet component. Consequently, this energy is used as a damage index. In further steps, damage is classified by means of fuzzy clustering. As a final phase, damage is identified using a vector machine. The numerical example illustrated in this work shows that the proposed method is able to identify the damage from the spatial truss structure. In 2011, Chen and Zang [8] presented an algorithm based on immune network theory and hierarchical clustering algorithms. Chilengue et al. [9] presented an artificial immune system (AIS) approach to detect and diagnose failures in the stator and rotor circuits of an induction machine. In the approach, the dynamic of the machine is compared before and after the fault condition. Similarly, the alpha-beta ($\alpha\beta\gamma$) transformation (also known as the Clarke transformation) was applied to the stator current to obtain a characteristic pattern of the machine that is finally applied to the pattern recognition algorithm.

In 2012, Zhou et al. [10], inspired by Chen's work, developed a damage classifier in structures based on the immune principle of clonal selection. Using evolution algorithms and the immune learning, a high quality memory cell is created that is able to identify several damage patterns. In 2012, Xiao [11] developed a structural health monitoring and fault diagnosis system based on artificial immune system. In this approach, the antigen represents the structural state (health or damage), whereas the antibody represents database information to identify a damage pattern. In this work, the feature space is formed by natural frequencies and modal shapes collected by simulation of the structure in free vibration and seismic response. Quite recently, Liu et al. [12], in 2014, proposed a structural damage detection method using semisupervised fuzzy *c*-means clustering method, wavelet packet decomposition, and data fusion. This method is applied to detect damage in a four-level benchmark model. The data that was used includes 11 damage patterns and 9 samples per damage. The method uses a Daubechies wavelet filter and 6 decompositions levels. According to the results, the method can achieve a reasonable detection performance. Huang et al. [13], in 2014, proposed an automatic methodology to know the status of a machine. The introduced method includes a semisupervised fuzzy-based method to detect the faults or

anomalies in the machine and to classify the unknown faults. The authors described two steps for the learning procedure as follows: (i) a fuzzy c-means clustering to get candidates of labels (fuzzy centers) and (ii) a label matching by filtering out the unreasonable labels candidates. The proposed method is validated in a roller bearing test top diagnosing the state of the machine.

Compared with the works previously reviewed, the methodology described on the current work presents a new point of view, since this uses an artificial immune system (AIS) and some damage indices to define feature vectors which represents the structure under different conditions by allowing the fact that the damage detection process can be understood as a pattern recognition approach. More precisely, damage detection and classification using ultrasonic signals have been traditionally performed using methods based on the time of flight. The approach followed in this paper, which complements and completes the initial work by Anaya et al. [14], is rather different because it is a data-based approach based on AIS (artificial immune system), where sensor data fusion, feature extraction, and pattern recognition are evaluated. A clear major advantage of the methodology is that the development and validation of a mathematical model are not needed. Additionally and in contrast to standard Lamb waves-based methods there is no necessity of directly analyzing the complex time-domain traces containing overlapping, multimodal, and frequency dispersive wave propagation which distorts the signals and makes their analysis difficult. However, using the proposed methodology, it is not possible to provide a multidamage detection able to identify several occurring damage patterns independently unless the model baselines are built with the structural responses that have interacted with previously detected and existing damage.

This paper is organized as follows. Section 2 describes the theoretical background that includes basic concepts about the methods and elements used in the methodology. Section 3 includes the damage detection methodology followed by the description about the experimental setup in Section 4. The experimental results are included in Section 5. Finally, some conclusions are drawn.

2. General Framework

The current work is based on data-driven analysis. This means that the damage detection will be developed by analyzing and interpreting the data collected in several experiments from the structures under diagnosis. To perform this analysis, a bioinspired methodology based on features extraction for pattern recognition is developed. For the sake of clarity, basic concepts and fundamentals about the methods that will be used are presented in the following subsections.

2.1. Bioinspired Systems. The adaptation of the different living beings of the planet in harsh environments and the development of skills to solve the inherent problems in the interaction with the world of nature have resulted in the evolution of the species in order to survive and avoid their extinction. Some examples are the communication abilities, the reasoning, the physical structures design, or the response of the body to external agents, among others [15].

Taking advantage of the fact that nature provides robust and efficient solutions to many different problems, more and more researchers on different areas work in the development of biologically inspired hardware and algorithms. The inspiration process is called *biomimetic* or *bioinspired* and aims to apply the developments in the field of biology to the engineering developments [16].

2.2. Natural Immune Systems. The human immune system (HIS) is a complex and robust defense mechanism composed of a large network of specialized cells, tissues, and organs. The system further includes an elevated number of sensors and a high processing capability. The human immune system has proved its effectiveness in the detection of foreign elements by protecting the organism against disease. The principal skills of the human immune system are as follows:

(i) to discriminate between its own cells (self) and foreign cells (non-self);

(ii) to recognize different invaders (called antigens) in order to ensure the protection of the body;

(iii) to learn from specific antigens and adapt to them in order to improve the immune response to this kind of invader.

In general, when a foreign particle wants to gain access to the organism, it has to break several defense levels provided by the immune system that protects the organism. The idea of several defense levels is illustrated in Figure 1. These levels can be summarized as follows [17].

(i) *External Barriers.* These are the first and the major line of defense into the human body. This level can include elements such as the skin, the mucus secreted by the membranes, the tears, the saliva, and the urine. All of these elements present different physiological conditions that are harmful to the antigens, as the temperature or the pH level, among others. The response of these barriers is equal for any foreign invader [18].

(ii) *Innate Immune System.* This barrier refers to the defense mechanisms that are activated immediately or within a short lapse of time of an antigen's arrival in the body. The innate immune system operates when the first barrier has been broken This system, in opposition to the adaptive immune system, is not adaptive [17].

(iii) *Adaptive Immune System.* This is the last defense level and reacts to the stimulus of foreign cells or antigens that evade both the external barriers and the innate immune defense [17]. Adaptive immunity creates some sort of memory that leads to an improved response to future encounters with this antigen.

With respect to different type of cells, the immune system includes cells born in the bone marrow that are usually called *white blood cells*, *leukocytes*, or *leucocytes* [19]. Among

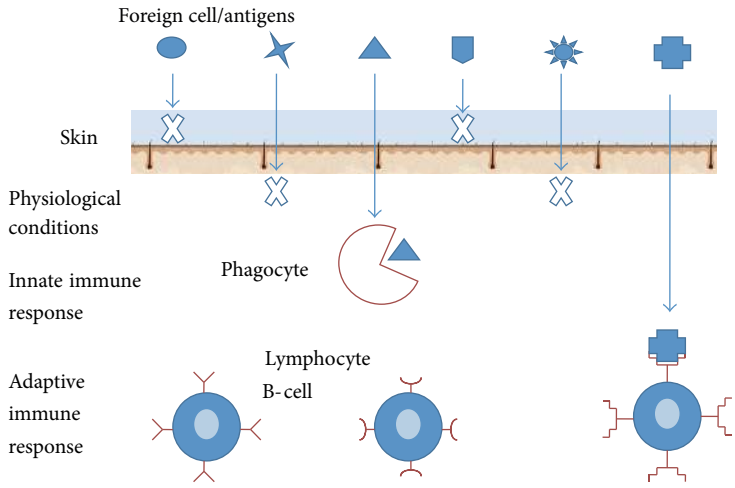

Figure 1: Schematic representation of a system's defense barriers.

the white blood cells, it is possible to highlight the T-cells and the B-cells. On the one hand, the T-cells are called so since their maturation takes place in the thymus. Besides, this kind of cells has high mobility and can also be found in the blood and the lymph [20]. One can distinguish three types of T-cells as follows:

(i) the T-helper cells, involved in the activation of B-cells;

(ii) the T-killer cells that destroy the invaders; and finally

(iii) the T-suppressor cells that avoid the allergic reactions [21].

On the other hand, the B-cells produce and secrete a special protein called antibody, which recognizes and binds the antigen. The responsibility of each B-cell is the production of a specific antibody. This protein is then used for signaling other cells whose elements have to be removed from the body [20]. When the antigen passes over the first barrier of the immune system, the HIS performs the following steps to eliminate the invader [20].

(1) The specialized cells of the immune system are called *antigen presenting cells* (APCs) (e.g., macrophages). These cells activate the immune response by ingesting the antigen and dividing it into simple substances known as antigenic peptides.

(2) These peptides are joined to the molecules called *major histocompatibility complex* (MHC), inside of the macrophage, and the result passes to the immune cell surface.

(3) The T-cells have receptor molecules able to identify and recognize different combinations of MHC-peptide. When the receptor molecule recognizes the combination, the T-cell is activated and sends a chemical signal to other immune cells.

(4) The B-cells are activated by chemical signals and they initiate the recognition of the antigen in the bloodstream. This process is performed by the receptor molecules in the B-cells.

(5) The mission of the B-cells, when they are activated, is to secrete antibodies to bind the antigens they find and to neutralize and eliminate them from the body.

The T- and B-cells that have recognized the antigen proliferate and some of them become memory cells. These memory cells remain in the immune system to eliminate the same antigen, in the future, in a more effective manner [15, 20].

Three immunological principles are used in artificial immune systems [11, 15, 20] as follows.

(i) *Immune Network Theory.* This theory was first introduced by Niels Jerne in 1974 and describes how the immune memory is built by means of the dynamic behaviour of the immune system cells. These cells can recognized by themselves, detect invaders, and interconnect between them to stabilize the network [17].

(ii) *The Negative Selection.* The negative selection is a process that allows the identification and eradication of the cells that react to their own body cells. This ensures a convenient operation of the immune system since it is able to distinguish between foreign molecules and self-molecules, thus avoiding autoimmune diseases. This process is similar to the maturation of T-cells carried out in the thymus [15].

(iii) *The Clonal Selection.* This is a mechanism of the adaptive immune responses in which the cells of the system are adapted to identify an invader element [20]. Antibodies that are able to recognize or identify an antigen can proliferate. Those antibodies unable to recognize the antigens are eliminated. The new cells are clones of their parents and they are subjected to an adaptation process by mutation. From the new antibody set, the cells with the greatest affinity with respect to the primary antigen are selected as memory cells, therefore excluding the rest.

Table 1: Analogy between the biological immune system and artificial immune system [11].

Biological immune system	Artificial immune system in SHM
Antibodies	A detector of a specific pattern
Antigens	Structural health or damage condition
Matured antibodies	Database or information system for damage detection
Recognition of antigens	Identification of health and damage condition
Process of mutation	Training procedure
Immune memory	Memory cells

2.3. Artificial Immune Systems. Artificial immune systems (AIS) are an adaptive and bioinspired computational systems based on the processes and performance of the human immune system (HIS) and its properties, diversity, error tolerance, dynamic learning, adaptation, distributed computation, and self-monitoring [22, 23]. Nowadays, these computational systems are used in several research areas such as pattern recognition [16], optimization [20, 24], and computer security [25] [26]. Table 1 presents the analogy between the natural and artificial immune systems applied to the field of structural health monitoring.

In the implementation of an artificial immune system, it is fundamental to bear in mind two important aspects as follows.

(i) The first is to define the role of the antigen (ag) and the antibody (ab) in the context of the application. Both are represented or coded in the same way. This representation is generally given by a vector of binary or real numbers [21].

(ii) The second is to define the mechanism that measures the degree of correspondence between an antigen and an antibody. This measure is usually related to the distance between them [15]. If both an antigen and an antibody are represented by L-dimensional arrays,

$$\begin{aligned} \mathrm{ab} &\in \mathbb{R}^L, \\ \mathrm{ag} &\in \mathbb{R}^L, \end{aligned} \tag{1}$$

the distance d between them can be computed using, for instance, the Euclidean distance (related to the 2-norm) or the so-called Manhattan distance (related to the 1-norm) as in the following equations, respectively [19]:

$$d(\mathrm{ab}, \mathrm{ag}) = \|\mathrm{ab} - \mathrm{ag}\|_2 = \sqrt{\sum_{i=1}^{L} (\mathrm{ab}_i - \mathrm{ag}_i)^2}, \tag{2}$$

$$d(\mathrm{ab}, \mathrm{ag}) = \|\mathrm{ab} - \mathrm{ag}\|_1 = \sum_{i=1}^{L} |\mathrm{ab}_i - \mathrm{ag}_i|. \tag{3}$$

Finally, there exists the adaptation process of the molecules in the artificial immune system. This adaptation allows including the dynamic of the system, for instance, the antibodies excitation, cloning of all the excited antibodies, and the interconnection between them. All these elements are adapted from the three immunologic principles previously introduced.

2.4. Principal Component Analysis (PCA). Principal component analysis (PCA) is a classical method used in applied multivariate statistical analysis with the goal of dimensionality reduction and, more precisely, feature extraction and data reduction. It was developed by Karl Pearson in 1901 and integrated to the mathematical statistics in 1933 by Harold Hotelling [27]. The general idea in the use of PCA is to find a smaller set of variables with less redundancy [28]. To find these variables, the analysis includes the transformation of the current coordinate space to a new space to reexpress the original data trying to filter the noise and redundancies. These redundancies are measured by means of the correlation between the variables.

2.4.1. Matrix Unfolding. The application of PCA starts, for each actuation phase, with the collected data arranged in a three-dimensional matrix $n \times L \times N$. The matrix is subsequently unfolded, as illustrated in Figure 2, in a two-dimensional $n \times (N \cdot L)$ matrix as follows:

$$\mathbf{X} = \begin{pmatrix} x_{11}^1 & x_{12}^1 & \cdots & x_{1L}^1 & x_{11}^2 & \cdots & x_{1L}^2 & \cdots & x_{11}^N & \cdots & x_{1L}^N \\ \vdots & \vdots & \ddots & \vdots & \vdots & \ddots & \vdots & \ddots & \vdots & \ddots & \vdots \\ x_{i1}^1 & x_{i2}^1 & \cdots & x_{iL}^1 & x_{i1}^2 & \cdots & x_{iL}^2 & \cdots & x_{i1}^N & \cdots & x_{iL}^N \\ \vdots & \vdots & \ddots & \vdots & \vdots & \ddots & \vdots & \ddots & \vdots & \ddots & \vdots \\ x_{n1}^1 & x_{n2}^1 & \cdots & x_{nL}^1 & x_{n1}^2 & \cdots & x_{nL}^2 & \cdots & x_{n1}^N & \cdots & x_{nL}^N \end{pmatrix}. \tag{4}$$

Matrix $\mathbf{X} \in \mathscr{M}_{n\times(N\cdot L)}(\mathbb{R})$, where $\mathscr{M}_{n\times(N\cdot L)}(\mathbb{R})$ is the vector space of $n \times (N \cdot L)$ matrices over $\mathbb{R}$, contains data from N sensors at L discretization instants and n experimental trials [29]. Consequently, each row vector $x_i^T = \mathbf{X}(i,:) \in \mathbb{R}^{N\cdot L}$, $i = 1, \ldots, n$, represents, for a specific experimental trial, the measurements from all the sensors. Equivalently, each column vector $\mathbf{X}(:, j) \in \mathbb{R}^n$, $j = 1, \ldots, N \cdot L$, represents measurements from one sensor in the whole set of experimental trials.

In other words, the objective is to find a linear transformation orthogonal matrix $\mathbf{P} \in \mathscr{M}_{(N\cdot L)\times(N\cdot L)}(\mathbb{R})$ that will be used to transform the original data matrix $\mathbf{X}$ according to the following matrix multiplication:

$$\mathbf{T} = \mathbf{X}\mathbf{P} \in \mathscr{M}_{n\times(N\cdot L)}(\mathbb{R}). \tag{5}$$

Matrix $\mathbf{P}$ is usually called the principal components of the data set or loading matrix and matrix $\mathbf{T}$ is the transformed or projected matrix to the principal component space, also called score matrix. Using all the $N \cdot L$ principal components, that is, in the full dimensional case, the orthogonality of $\mathbf{P}$

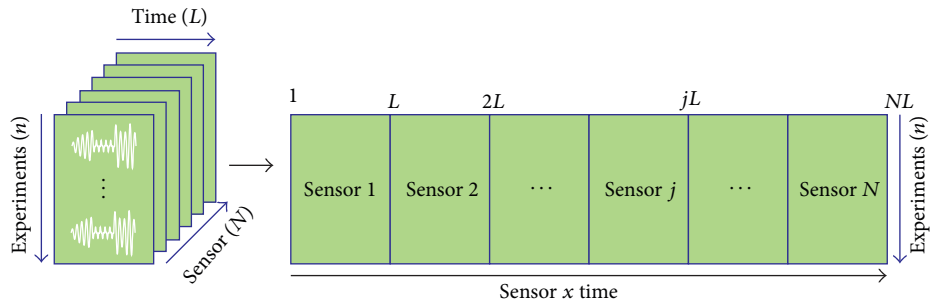

FIGURE 2: The collected data arranged in a three-dimensional matrix is unfolded in a two-dimensional matrix [30].

implies $\mathbf{P}\mathbf{P}^T = \mathbf{I}$, where $\mathbf{I}$ is the $(N \cdot L) \times (N \cdot L)$ identity matrix. Therefore, the projection can be inverted to recover the original data as

$$\mathbf{X} = \mathbf{T}\mathbf{P}^T. \tag{6}$$

2.4.2. Group Scaling. Since the data in matrix $\mathbf{X}$ come from experimental trials and could have different magnitudes and scales, it is necessary to apply a preprocessing step to scale the data using the mean of all measurements of the sensor at the same time and the standard deviation of all measurements of the sensor [29].

More precisely, for $k = 1, 2, \ldots, N$, we define

$$\mu_j^k = \frac{1}{n}\sum_{i=1}^{n} x_{ij}^k, \quad j = 1, \ldots, L, \tag{7}$$

$$\mu^k = \frac{1}{nL}\sum_{i=1}^{n}\sum_{j=1}^{L} x_{ij}^k, \tag{8}$$

$$\sigma^k = \sqrt{\frac{1}{nL}\sum_{i=1}^{n}\sum_{j=1}^{L}\left(x_{ij}^k - \mu^k\right)^2}, \tag{9}$$

where μ_j^k is the mean of the n measures of sensor k at the time instant j; μ^k is the mean of all the measures of sensor k; and σ^k is the standard deviation of all the measures of sensor k. Therefore, the elements x_{ij}^k of matrix $\mathbf{X}$ are scaled to define a new matrix $\check{\mathbf{X}}$ as

$$\check{x}_{ij}^k := \frac{x_{ij}^k - \mu_j^k}{\sigma^k}, \quad i = 1, \ldots, n,\ j = 1, \ldots, L,\ k = 1, \ldots, N. \tag{10}$$

When the data are normalized using (10), the scaling procedure is called *variable scaling* or *group scaling* [29]. According to former studies of the authors [30–32], group scaling presents a better performance than other kind of normalizations. The reason is that group scaling considers changes between sensors and does not process them independently. Further discussion on this issue can be found in [29, 33].

For simplicity and throughout the rest of the paper the scaled matrix $\check{\mathbf{X}}$ is renamed as simply $\mathbf{X}$. The mean of each column vector in the scaled matrix $\mathbf{X}$ can be computed as

$$\begin{aligned}\frac{1}{n}\sum_{i=1}^{n}\check{x}_{ij}^k &= \frac{1}{n}\sum_{i=1}^{n}\frac{x_{ij}^k - \mu_j^k}{\sigma^k} = \frac{1}{n\sigma^k}\sum_{i=1}^{n}\left(x_{ij}^k - \mu_j^k\right)\\ &= \frac{1}{n\sigma^k}\left(\sum_{i=1}^{n} x_{ij}^k - n\mu_j^k\right) = \frac{1}{n\sigma^k}\left(n\mu_j^k - n\mu_j^k\right)\\ &= 0.\end{aligned} \tag{11}$$

Since the scaled matrix $\mathbf{X}$ is a *mean-centered* matrix, it is possible to calculate the covariance matrix as follows:

$$\mathbf{C}_\mathbf{X} = \frac{1}{n-1}\mathbf{X}^T\mathbf{X} \in \mathscr{M}_{(N\cdot L)\times(N\cdot L)}(\mathbb{R}). \tag{12}$$

The covariance matrix $\mathbf{C}_\mathbf{X}$ is $(N\cdot L)\times(N\cdot L)$ symmetric matrix that measures the degree of linear relationship within the data set between all possible pairs of variables (sensors).

The subspaces in PCA are defined by the eigenvectors and eigenvalues of the covariance matrix as follows:

$$\mathbf{C}_\mathbf{X}\mathbf{P} = \mathbf{P}\Lambda, \tag{13}$$

where the columns of $\mathbf{P} \in \mathscr{M}_{(N\cdot L)\times(N\cdot L)}(\mathbb{R})$ are the eigenvectors of $\mathbf{C}_\mathbf{X}$. The diagonal terms of matrix $\Lambda \in \mathscr{M}_{(N\cdot L)\times(N\cdot L)}(\mathbb{R})$ are the eigenvalues λ_i, $i = 1, \ldots, N \cdot L$, of $\mathbf{C}_\mathbf{X}$ whereas the off-diagonal terms are zero; that is,

$$\begin{aligned}\Lambda_{ii} &= \lambda_i, \quad i = 1, \ldots, N \cdot L,\\ \Lambda_{ij} &= 0, \quad i, j = 1, \ldots, N \cdot L,\ i \neq j.\end{aligned} \tag{14}$$

The eigenvectors p_j, $j = 1, \ldots, N\cdot L$, representing the columns of the transformation matrix $\mathbf{P}$, are classified according to the eigenvalues in descending order and they are called the *principal components* or the *loading vectors* of the data set. The eigenvector with the highest eigenvalue, called the *first principal component*, represents the most important pattern in the data with the largest quantity of information.

However, the objective of PCA is, as said before, to reduce the dimensionality of the data set $\mathbf{X}$ by selecting only a limited number $\ell < N \cdot L$ of principal components, that is, only the eigenvectors related to the ℓ highest eigenvalues. Thus, given the reduced matrix

$$\widehat{\mathbf{P}} = \left(p_1 \mid p_2 \mid \cdots \mid p_\ell\right) \in \mathscr{M}_{N\cdot L\times \ell}(\mathbb{R}), \tag{15}$$

matrix $\widehat{\mathbf{T}}$ is defined as

$$\widehat{\mathbf{T}} = \mathbf{X}\widehat{\mathbf{P}} \in \mathscr{M}_{n\times \ell}(\mathbb{R}). \tag{16}$$

Note that opposite to $\mathbf{T}$, $\widehat{\mathbf{T}}$ is no longer invertible. Consequently, it is not possible to fully recover $\mathbf{X}$ although $\widehat{\mathbf{T}}$ can be projected back onto the original m-dimensional space to get a data matrix $\widehat{\mathbf{X}}$ as follows:

$$\widehat{\mathbf{X}} = \widehat{\mathbf{T}}\widehat{\mathbf{P}}^T \in \mathscr{M}_{n\times m}(\mathbb{R}). \tag{17}$$

The difference between the original data matrixes $\mathbf{X}$ and $\widehat{\mathbf{X}}$ is defined as the *residual error matrix* $\mathbf{E}$ or $\widetilde{\mathbf{X}}$ as follows:

$$\mathbf{E} = \mathbf{X} - \widehat{\mathbf{X}}, \tag{18}$$

or, equivalently,

$$\mathbf{X} = \widehat{\mathbf{X}} + \mathbf{E} = \widehat{\mathbf{T}}\widehat{\mathbf{P}}^T + \mathbf{E}. \tag{19}$$

The residual error matrix $\mathbf{E}$ describes the variability not represented by the data matrix $\widehat{\mathbf{X}}$ and can be also expressed as

$$\mathbf{E} = \mathbf{X}\left(\mathbf{I} - \widehat{\mathbf{P}}\widehat{\mathbf{P}}^T\right). \tag{20}$$

Even though the real measures obtained from the sensors as a function of time represent physical magnitudes, when these measures are projected and the scores are obtained, these scores no longer represent any physical magnitude [34].

2.5. Damage Detection Indices Based on PCA. Several damage detection indices based on PCA have been proposed and applied with excellent results in pattern recognition applications. In particular, two damage indices are commonly used: (i) the Q index (also known as SPE, *square prediction error*) and (ii) Hotelling's T^2 index.

The Q index of the ith experimental trial x_i^T measures the magnitude of the vector $\widetilde{x}_i^T := \widetilde{\mathbf{X}}(i,:)$, that is, the events that are not explained by the model of principal components [35], and it is defined as follows:

$$Q_i = \widetilde{\mathbf{X}}(i,:)\,\widetilde{\mathbf{X}}(i,:)^T = x_i^T\left(\mathbf{I} - \widehat{\mathbf{P}}\widehat{\mathbf{P}}^T\right)x_i. \tag{21}$$

The T^2 index of the ith experimental trial x_i^T is the weighted norm of the projected vector $\widehat{t}_i^T := \widehat{\mathbf{T}}(i,:) = x_i^T\widehat{\mathbf{P}}$, that is, a measure of the variation of each sample within the PCA model, and it is defined as follows:

$$T_i^2 = \sum_{j=1}^{\ell}\frac{\widehat{t}_{i,j}^2}{\lambda_j} = \widehat{t}_i^T\Lambda^{-1}\widehat{t}_i = x_i^T\left(\widehat{\mathbf{P}}\Lambda^{-1}\widehat{\mathbf{P}}^T\right)x_i. \tag{22}$$

3. Damage Detection Methodology

The damaged detection methodology that we present in this paper involves an active piezoelectric system to inspect the structure. This active system consists of several piezoelectric transducers (lead zirconium titanate, PZT) distributed on different positions of the structure and working as both actuators or sensors in different actuation phases. Each PZT is able to produce a mechanical vibration if some electrical excitation is applied (actuator mode). Besides, the PZTs are able to detect time varying mechanical response data (sensor mode). In each phase of the experimental stage, just one PZT is used as the actuator (exciting the structure). Then, the propagated signal through the structure is collected by using the rest of PZTs, which are used as sensors. This procedure is repeated in as many actuation phases as the number of PZTs on the structure.

To determine the presence of damage in the structure, the data from each actuation phase will be used in the proposed artificial immune system. The proposed methodology is performed in three steps as follows: (i) data preprocessing and feature extraction; (ii) training process; and (iii) testing. More precisely, in the first step the collected data is organized, preprocessed, and dimensionally reduced, by means of principal component analysis, to obtain relevant information. The damage indices in (21)-(22) are used to define the feature vectors. The training step includes the evolution of the data to *generate* good representatives for each pattern, damage, or structural condition. A good accuracy in the damage detection using AIS depends on a good training. Finally, the testing step includes new data to evaluate the training step and the knowledge of the current state of the structure.

3.1. Data Preprocessing, PCA Modeling, and Feature Extraction. For each different phase (PZT1 will act as an actuator in phase 1, PZT2 will act as an actuator in phase 2, and so on) and considering the signals measured by the sensors, the matrix $\mathbf{X}$ is defined and arranged as in (4) in Section 2.4.1 and scaled as stated in Section 2.4.2. PCA modeling basically consists of computing the projection matrix $\mathbf{P}$ for each phase as in (7). Matrix $\mathbf{P}$, renamed as $\mathbf{P}_{\text{model}}$, provides an improved and dimensionally limited representation of the original data $\mathbf{X}$. The number of principal components retained at each different phase accounts for at least 90% of the cumulative variance.

Subsequently, the data from different structural states are projected into each PCA model in order to obtain the scores and calculate the damage detection indices T^2 and Q as in Sections 2.4 and 2.5. In this way, for each experiment, a two-dimensional *feature vector*

$$f^i = \left(T_i^2, Q_i\right)^T \in \mathbb{R}^2, \quad i = 1, \ldots, \nu \tag{23}$$

is defined, where ν is the total number of experiments. The feature vector could include more components, as, for instance, the scores. Several tests were then performed in this sense with the combination of scores and damage indices. However, the results indicated that the single use of T^2 and

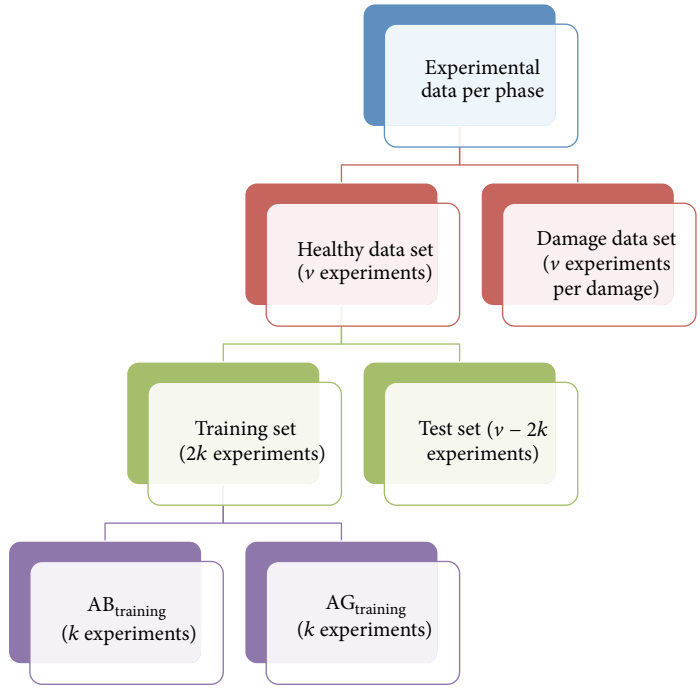

Figure 3: Random selection of the antibody ($AB_{training}$) and antigen ($AG_{training}$) training sets.

Q leads to the best results. One of the reasons about the use of the damage indices can be found in [35]. In this paper, Tibaduiza et al. showed that the use of scores is not sufficient for damage detection when two scores do not account for a high cumulative variance. This result implies that it is necessary to use another type of measurement or statistic to obtain an accurate discrimination of the presence of damage in a structure.

To keep the affinity values within the range of $[0, 1]$, the norm of the feature vectors f_i, $i = 1, \ldots, \nu$, is normalized to the unit circle. The normalization process uses the maximum norm of the feature vectors; that is,

$$M := \max_{i=1,\ldots,\nu} \left\| f^i \right\|, \tag{24}$$

where

$$\left\| f^i \right\| = \sqrt{\left(f_1^i\right)^2 + \left(f_2^i\right)^2}, \tag{25}$$

and therefore the normalized feature vector f^i_{norm} of $f^i = (T_i^2, Q_i)^T$ is as follows:

$$f^i_{\text{norm}} = \left(\frac{T_i^2}{M}, \frac{Q_i}{M} \right). \tag{26}$$

Since all the feature vectors are located within a unit circle, the Euclidean distance between any feature vectors is less than or equal to 2. The *healthy data set* (HDS) is defined as

$$\text{HDS} = \bigcup_{i=1}^{\nu} \left\{ f^i \right\}. \tag{27}$$

3.2. Training Step. This step can be modified according to different goals. For instance, in the most basic case in damage identification, the detection, the training only needs to consider the feature vectors that come from data of the healthy structure. However, in a more complex analysis, the classification, for instance, the training process must include the feature vectors of data coming from the structure in different and known structural states. The steps to perform the training in the basic case are summarized as follows:

(i) Randomly select $2k \in \mathbb{N}$, $2k < \nu$, feature vectors. The remaining $\nu - 2k$ feature vectors will be used in the testing process. This set of $2k$ feature vectors is divided into two subsets of the same size k, the *antibody training set* ($AB_{training}$) and the *antigen training set* ($AG_{training}$). This step is represented in Figure 3.

(ii) Compute the affinity between the antibodies and antigens of the $AB_{training}$ and $AG_{training}$ sets, respectively. The affinity between an antibody and an antigen is defined as

$$\text{Aff}(\text{ab}, \text{ag}) := 1 - \frac{1}{2} d(\text{ab}, \text{ag}), \tag{28}$$

where $d(\text{ab}, \text{ag})$ is the distance, defined in (2), between the feature vectors of ab and ag, respectively. Since the Euclidean distance between any feature vectors is less than or equal to 2, their affinity lies within the range of $[0, 1]$.

(iii) Evolve the antibodies. The evolution of the antibodies is performed when these are stimulated by an invading antigen invader and it consists in the mutation of

the antibody. The mutation is performed by mutating the feature vectors of the cloned antibodies as shown in

$$\text{ab}_{\text{evolved}} = \text{ab} + \text{MV} \cdot \phi, \tag{29}$$

where $\text{ab}_{\text{evolved}}$ is the mutated antibody and MV represents the mutation value, a value used to indicate the mutation degree of the feature vector of an antibody. In the present implementation, the mutation value is defined as in

$$\text{MV} = 1 - \text{CV}, \tag{30}$$

where CV is the *clonal value*, a value that measures the response of an artificial B-cell to an antigen, and is equal to the affinity between the antibody and the stimulating antigen. The vector

$$\phi = \left(\phi_1, \phi_2\right)^T \in \mathbb{R}^2 \tag{31}$$

in (29) is a randomly generated vector. Each element ϕ_i, $i = 1, 2$, of the random vector is a normally distributed random variable with mean zero and standard deviation $\sigma = 0.5$.

The mutated antibody feature vectors must lie within the unit circle. Therefore, the norm of the feature vector for each mutated antibody is immediately checked after the mutation according to the following procedure:

(a) if $\|\text{ab}_{\text{evolved}}\| \leq 1$, then no normalization is performed;

(b) if $\|\text{ab}_{\text{evolved}}\| > 1$, then

$$\text{ab}_{\text{evolved}} = \left(\|\text{ab}\| + \mathcal{U} \cdot (1 - \|\text{ab}\|)\right) \cdot \frac{\text{ab}_{\text{evolved}}}{\left\|\text{ab}_{\text{evolved}}\right\|}, \tag{32}$$

where $\mathcal{U}$ is a uniform random function with a value within the range of $[0, 1]$.

The norm of the mutated antibody is greater than the norm of the original antibody and less than 1.

The *clonal rate* (CR) is an integer value used to control the number of antibody clones allowed. The number of clones (NC) is defined in

$$\text{NC} = \lfloor \text{CR} \cdot \text{CV} \rfloor, \tag{33}$$

where $\lfloor \cdot \rfloor$ is the floor function. In this paper the value of CR is 8.

The highest affinity antibody is chosen as the candidate memory cell for possible updating of memory cell set.

(iv) Define the threshold. A threshold T_h is defined in order to update the memory cell set to improve the representation quality of memory cells for the healthy state of the structure. This threshold is defined as a weighted affinity of the two elements in the healthy data set (HDS) in (27) with the maximum Euclidean distance. That is,

$$\begin{aligned} \Delta &= \max_{i,j=1,\ldots,n} \left\| f^i - f^j \right\|, \\ \delta &= \frac{7}{25}\Delta, \\ T_h &= 1 - \frac{1}{2}\delta. \end{aligned} \tag{34}$$

Then a comparison between the candidate memory cell and all the elements in the healthy data set (HDS) is performed through the affinity. If the affinities are greater than or equal to the threshold, the candidate memory cell becomes memory cell of the healthy state of the structure. Otherwise, the candidate memory cell is eliminated. The main outcome of this step is the *memory cell set* of the healthy state (MCSH) of the structure. This algorithmic training process is represented in Figure 4.

3.3. Testing Step. The damage detection algorithm is finally illustrated in Figure 5. The damage detection is based on the affinity values between the elements in the memory cell set of the healthy state (MCSH), acting as antibodies, and the data coming from the structure to test (TD, test data), acting as antigens. A *detection threshold* (D_{Th}) is defined in the following equation for this purpose:

$$D_{\text{Th}} = \min_{\substack{\text{ab} \in \text{MCSH} \\ i \in \{1,\ldots,\nu\}}} \text{Aff}\left(\text{ab}, f^i\right), \tag{35}$$

that is, the minimum affinity between the elements in the memory cell set of healthy state (MCSH) and the elements in the healthy data set (HDS).

When the affinity is less than the threshold D_{Th}, we say that the data has been collected from a damaged state of the structure. Otherwise, the data comes from an undamaged structure.

4. Experimental Setup and Experimental Results

4.1. Experimental Setup. To test the proposed methodology, data from an aircraft skin panel is used. The structure is divided into small sections by means of stringers and ribs as shown in Figure 6. To validate the proposed methodology, two sections of this structure were used. The dimensions of each section and the damage description are depicted in Figure 7. These sections were instrumented with 6 PZT transducers: two in the upper section, two in the lower section, and two in the rib. The transducers dimensions are as follows: 26 mm diameter and 0.4 mm thickness.

4.2. Experimental Results. As said in Section 3.1, the experiments are performed in 6 independent phases: (i) piezoelectric transducer 1 (PZT1) is configured as actuator and the rest

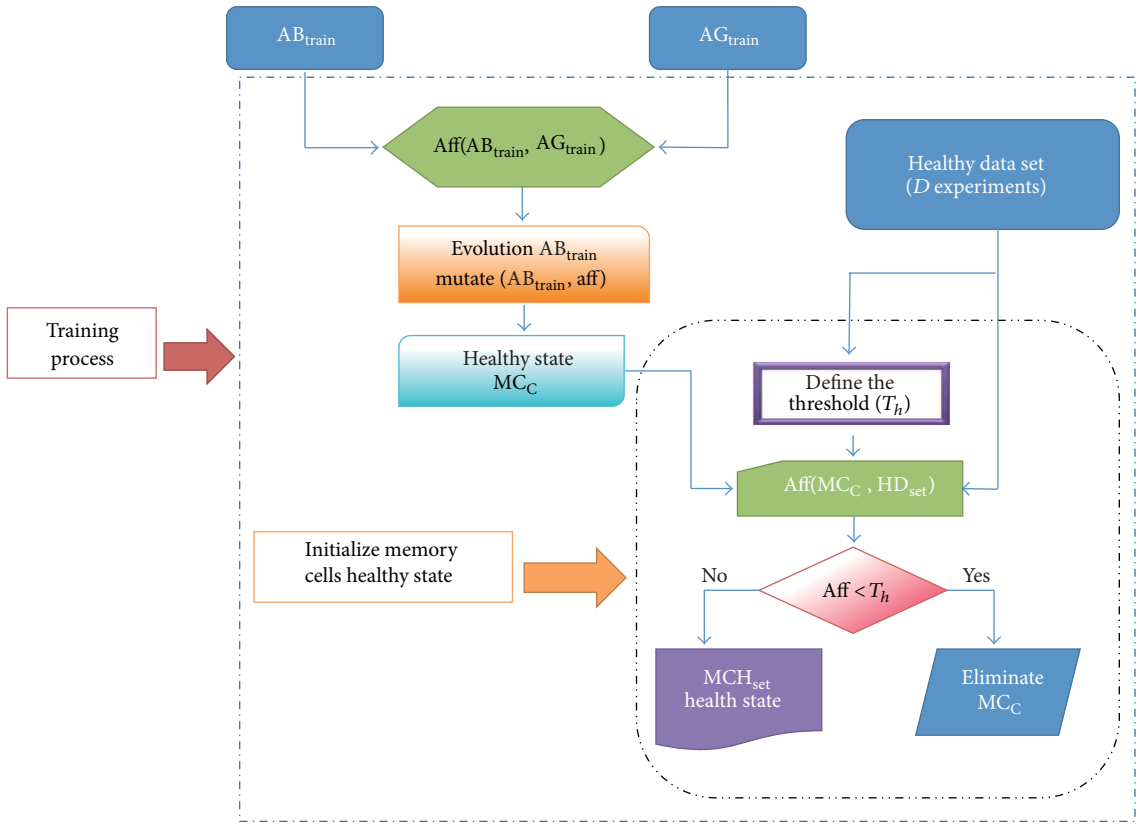

Figure 4: Training process in an artificial immune system (IAS) applied to structural health monitoring (SHM).

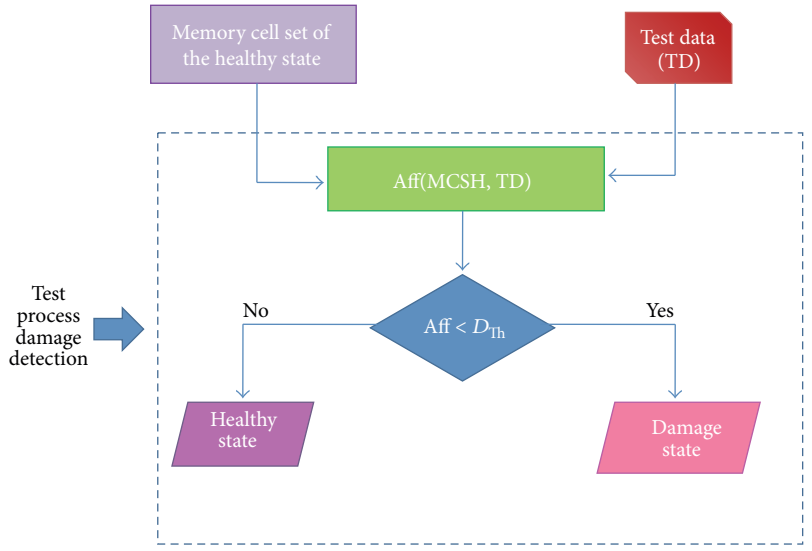

Figure 5: Damage detection process.

Figure 6: Aircraft skin panel.

of PZTs as sensors; (ii) PZT2 is configured as actuator; (iii) PZT3 is configured as actuator; (iv) PZT4 is configured as actuator; (v) PZT5 is configured as actuator; and (vi) PZT6 is configured as actuator.

To apply the proposed methodology and for each phase the collected data is arranged in a matrix as in (4) in Section 2.4.1. With this *unfolded* data, the PCA model **P** is

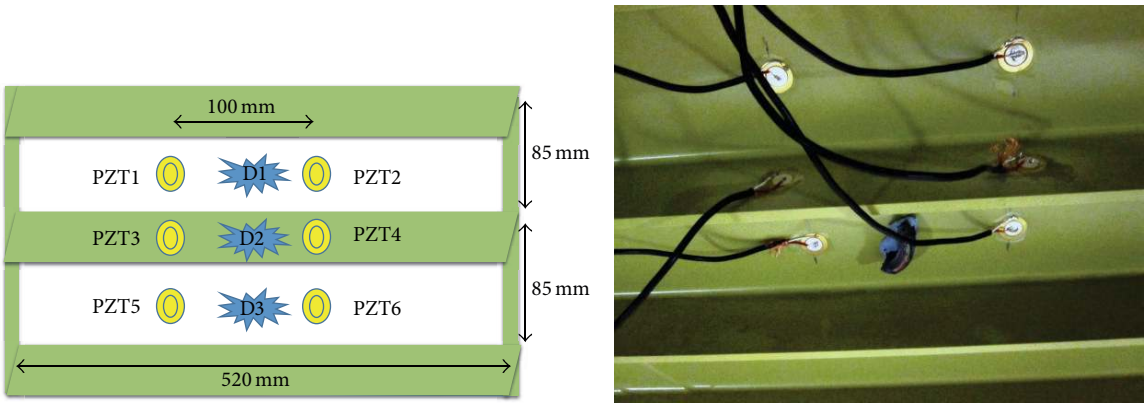

Figure 7: Damage description.

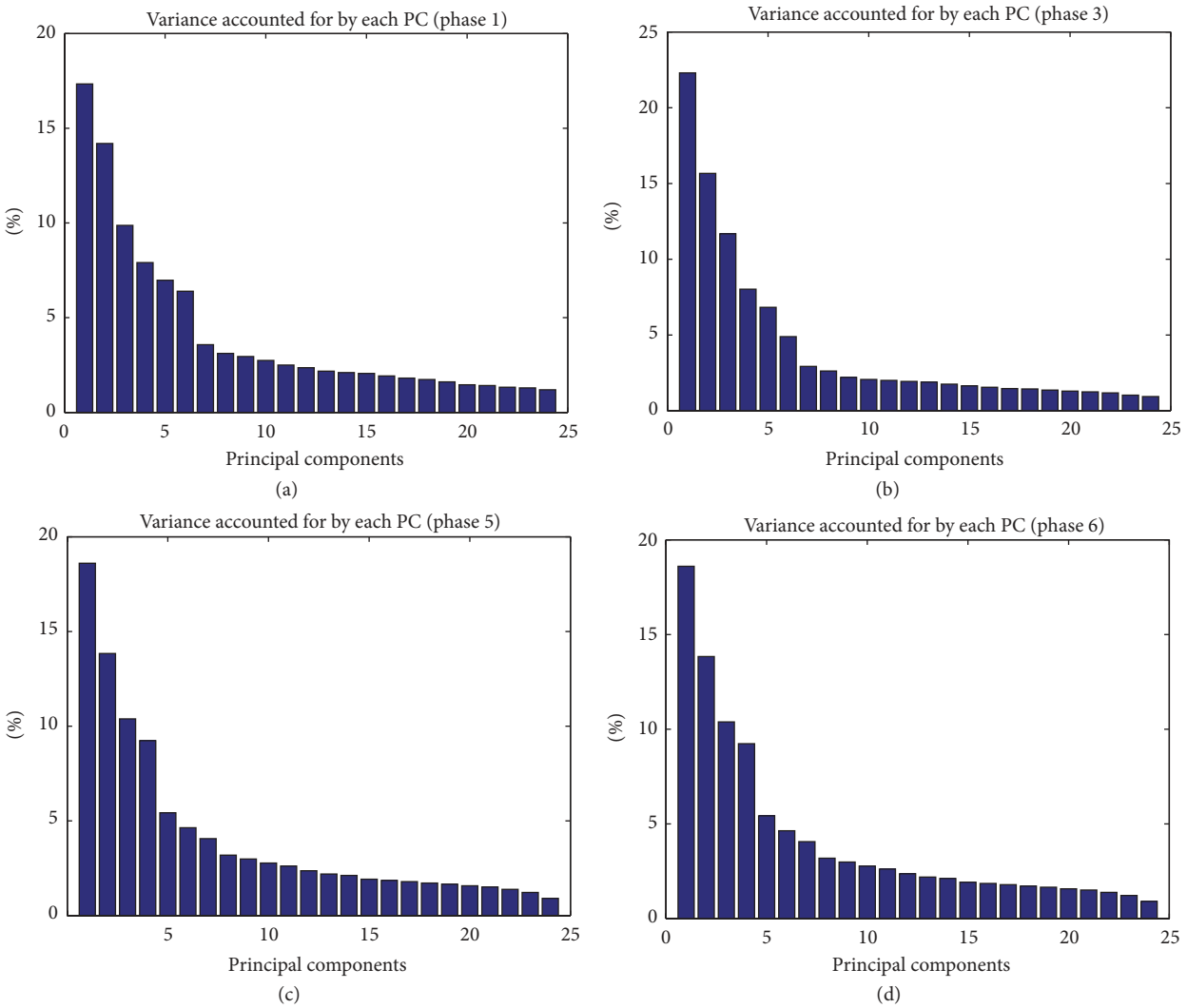

Figure 8: Amount of variance accounted for by each principal component, for phases 1, 3, 5, and 6.

built as explained in Sections 2.4 and 3.1 using data from the healthy structure. In Figure 8 the amount of variance accounted for by each principal component is illustrated, for phases 1, 3, 5, and 6.

For each actuator phase, the number of principal components adopted varies since the principal components retained must account for at least 90% of the cumulative variance. Although there is not an accurate criterion to state

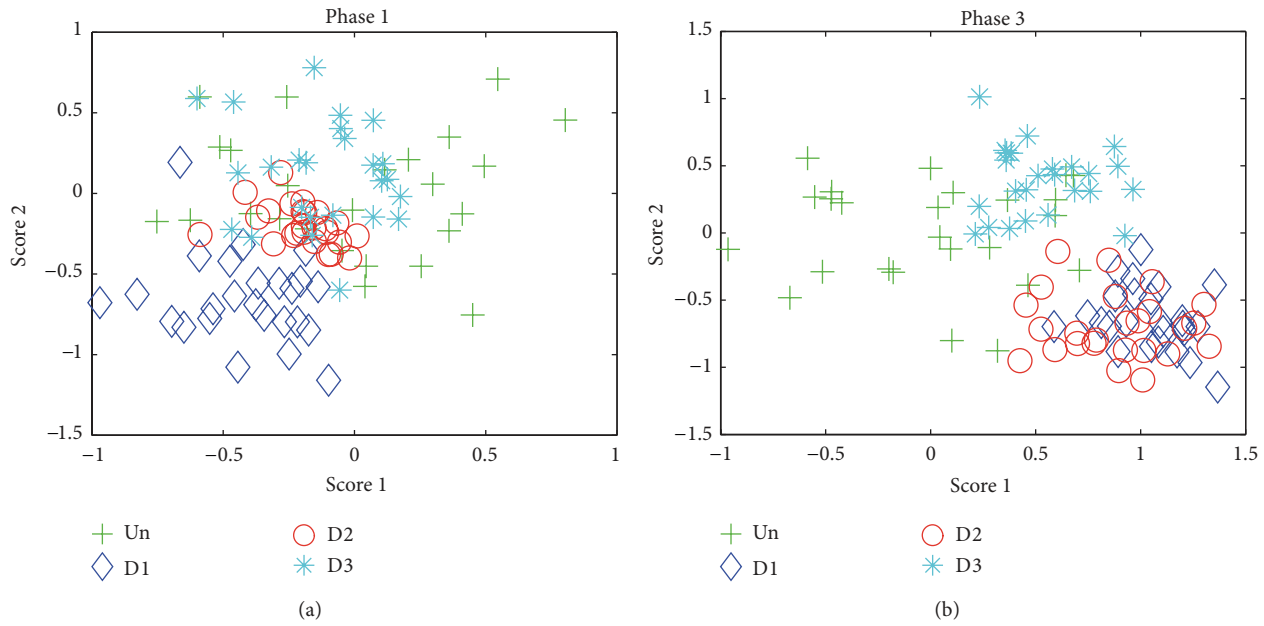

FIGURE 9: Projections onto the two first principal components of several experiments in actuator phases 1 (a) and 3 (b).

a percentage of cumulative variance to be retained for a good representation, a high percentage can ensure that most of the variability is incorporated into the statistical model.

Figure 9 shows the projections onto the two first principal components of several experiments that come from the undamaged and damaged structure under consideration. It can be clearly observed that no separation of damaged/undamaged can be determined using the scatter plot. These are then two motivating depictions in the sense that with the proposed methodology we will be able to both detect damage in the structure and classify it.

4.2.1. Damage Detection. After the baseline modeling, the data coming from the structure to be diagnosed is projected onto the PCA model. Then, for each experiment, the feature vector in (23) formed by the two damage indices T^2 and Q is defined.

The ability of the proposed method to detect damage in the structure is illustrated in Figures 10 to 15. In these figures, the affinity of a memory cell from the memory cell set of the healthy state (MCSH) and the data coming from the structure to diagnosis is depicted. The 25 first experiments correspond to data that come from the undamaged structure, while the remainder 75 experiments come from the damaged structure. More precisely, experiments 25 to 50 correspond to damage 1 ($D1$), experiments 51 to 75 to damage 2 ($D2$), and experiments 76 to 100 to damage 3 ($D3$). The purple solid horizontal line delimits the detection threshold (D_{Th}). It can be clearly observed that experiments with an affinity value less than D_{Th}, from the damaged structure, are correctly defined as "damaged." Similarly, experiments with an affinity value greater than or equal to D_{Th}, from the healthy structure, are correctly defined as "healthy."

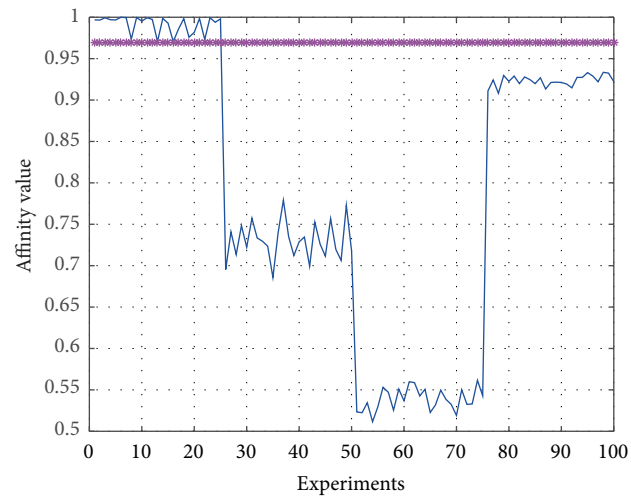

FIGURE 10: Affinity values between a memory cell of the memory cell set of the healthy state (MCSH) and the data coming from the structure to diagnosis (phase 1).

Actuation phases 1 to 5 show that it is possible to distinguish the healthy and unhealthy states; in addition it can be observed that different affinity values represent the differences between the group of data which indicate that it is possible to determine the presence of three damage patterns. In contrast to the affinity in the rest of the actuation phases, phase 6 in Figure 15 is showing that it is possible to detect abnormal situations; however it is not possible to determine the different structural states.

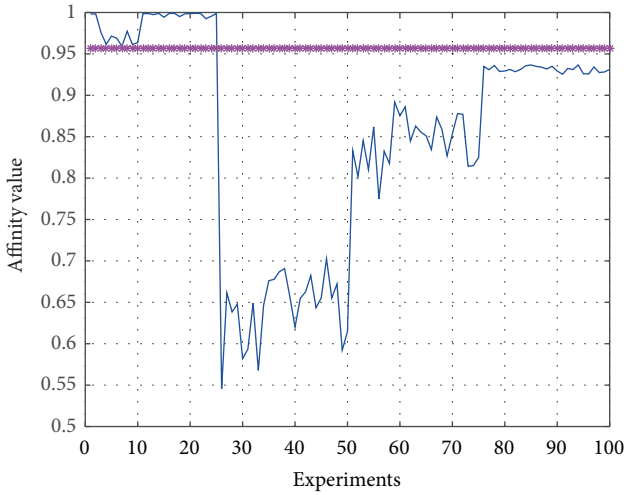

Figure 11: Affinity values between a memory cell of the memory cell set of the healthy state (MCSH) and the data coming from the structure to diagnosis (phase 2).

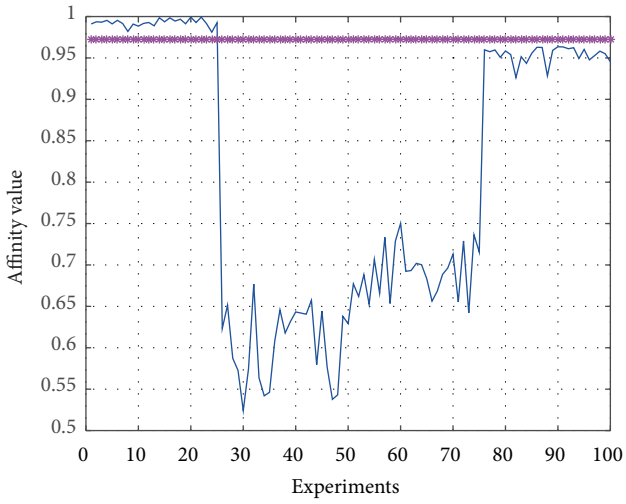

Figure 12: Affinity values between a memory cell of the memory cell set of the healthy state (MCSH) and the data coming from the structure to diagnosis (phase 3).

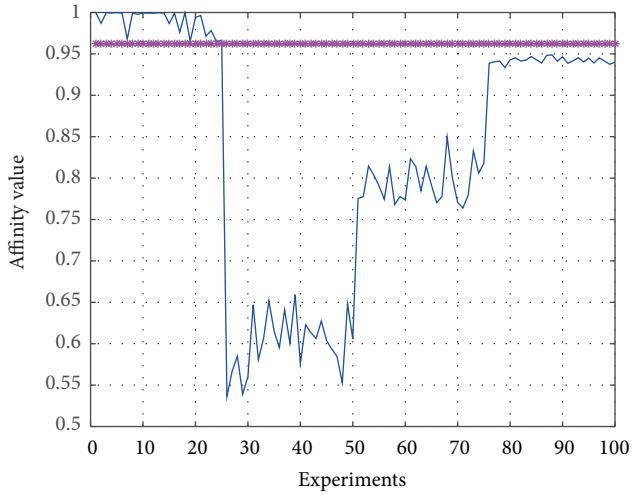

Figure 13: Affinity values between a memory cell of the memory cell set of the healthy state (MCSH) and the data coming from the structure to diagnosis (phase 4).

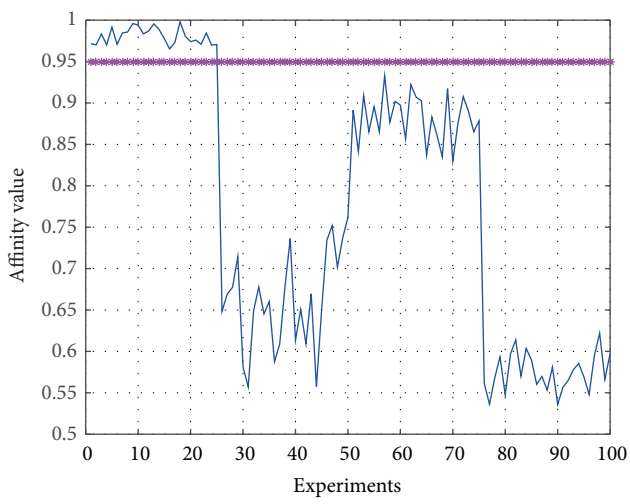

Figure 14: Affinity values between a memory cell of the memory cell set of the healthy state (MCSH) and the data coming from the structure to diagnosis (phase 5).

As it was shown, results from each actuation phase showed different affinity values to the different structural states; this is because the actuators are distributed by the structure in different positions and to different distance to the damage.

5. Concluding Remarks

In this paper, a new methodology to detect structural changes has been introduced. The methodology includes the use of an artificial immune system (AIS) and the notion of affinity for the damage detection.

One of the advantages of the methodology is the fact that to develop and validate a model is not needed. Additionally and in contrast to standard Lamb waves-based methods there is no need to directly analyze the complex time-domain traces containing overlapping, multimodal, and frequency dispersive wave propagation that distorts the signals and makes the analysis difficult. Results have shown that different actuation phases present different results.

The proposed methodology has been applied to data coming from two sections of an aircraft skin panel. The results indicate that the proposed methodology is able to accurately detect damage by means of the analysis of the affinity values. However, within the proposed methodology, it is not possible to provide a multidamage classification able to identify several simultaneous damage patterns. To ensure the proper performance of the methodology, a study of the

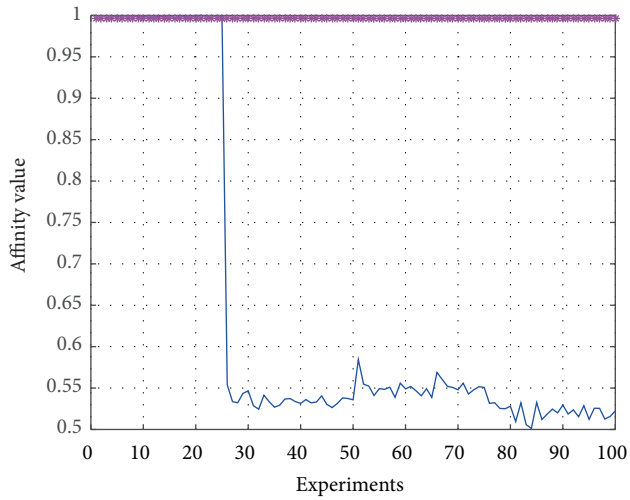

Figure 15: Affinity values between a memory cell of the memory cell set of the healthy state (MCSH) and the data coming from the structure to diagnosis (phase 6).

effect of changing environmental and operational conditions needs to be considered, which is considered as a future work. The methodology can be improved by applying data fusion in order to obtain an only plot with the information from the actuation phases. In this sense, the use of SOM or fuzzy clustering will allow the data fusion and estimate more information from the data.

Conflict of Interests

The authors declare that there is no conflict of interests regarding the publication of this paper.

Acknowledgments

This work is supported by CICYT (Spanish Ministry of Economy and Competitiveness) through Grants DPI2011-28033-C03-01 and DPI2014-58427-C2-1-R and by Universidad Santo Tomás through Grants FODEIN 2014, project code 047, and FODEIN 2015, project code 8410083003-036. The authors would also like to express their gratitude to the Professor Alfredo Güemes for providing the structure used in this paper and for his suggestions in the experimental setup and data acquisition process.

References

[1] P. J. C. Branco, J. A. Dente, and R. V. Mendes, "Using immunology principles for fault detection," *IEEE Transactions on Industrial Electronics*, vol. 50, no. 2, pp. 362–373, 2003.

[2] S. da Silva, M. Dias Jr., and V. Lopes Jr., "Damage detection in a benchmark structure using AR-ARX models and statistical pattern recognition," *Journal of the Brazilian Society of Mechanical Sciences and Engineering*, vol. 29, no. 2, pp. 174–184, 2007.

[3] S. da Silva, M. Dias Júnior, V. Lopes Junior, and M. J. Brennan, "Structural damage detection by fuzzy clustering," *Mechanical Systems and Signal Processing*, vol. 22, no. 7, pp. 1636–1649, 2008.

[4] J. Zhang, K. Worden, and W. J. Staszewski, "Sensor optimisation using an immune system metaphor," in *Proceedings of the 26th International Modal Analysis Conference (IMAC '08)*, 2008.

[5] J. R. Vieira de Moura Jr., S. Park, V. Steffen Jr., and D. J. Inman, "Fuzzy logic applied to damage characterization through SHM techniques," in *Proceedings of the International Modal Analysis Conference*, Society for Experimental Mechanics Series, 2008.

[6] B. Chen, "Agent-based artificial immune system approach for adaptive damage detection in monitoring networks," *Journal of Network and Computer Applications*, vol. 33, no. 6, pp. 633–645, 2010.

[7] D. Tan, W. Qu, and J. Tu, "The damage detection based on the fuzzy clustering and support vector machine," in *Proceedings of the International Conference on Intelligent System Design and Engineering Application (ISDEA '10)*, pp. 598–601, Changsha, China, October 2010.

[8] B. Chen and C. Zang, "Emergent damage pattern recognition using immune network theory," *Smart Structures and Systems*, vol. 8, no. 1, pp. 69–92, 2011.

[9] Z. Chilengue, J. A. Dente, and P. J. C. Branco, "An artificial immune system approach for fault detection in the stator and rotor circuits of induction machines," *Electric Power Systems Research*, vol. 81, no. 1, pp. 158–169, 2011.

[10] Y. Zhou, S. Tang, C. Zang, and R. Zhou, "An artificial immune pattern recognition approach for damage classification in structures," in *Advances in Information Technology and Industry Applications*, vol. 136 of *Lecture Notes in Electrical Engineering*, pp. 11–17, Springer, 2012.

[11] W. Xiao, *Structural health monitoring and fault diagnosis based on artificial immune system [Ph.D. thesis]*, Worcester Polytechnic Institute, 2012.

[12] Z. Liu, Q. Zhou, Q. Chi, Y. Zhang, Y. Chen, and S. Qi, "Structural damage detection based on semi-supervised fuzzy C-means clustering," in *Proceedings of the 9th International Conference on Computer Science & Education (ICCSE '14)*, pp. 551–556, IEEE, August 2014.

[13] Y. Huang, L. Gong, S. Wang, and L. Li, "A fuzzy based semi-supervised method for fault diagnosis and performance evaluation," in *Proceedings of the IEEE/ASME International Conference on Advanced Intelligent Mechatronics (AIM '14)*, pp. 1647–1651, Besançon, France, July 2014.

[14] M. Anaya, D. Tibaduiza, and F. Pozo, "Data-driven methodology based on artificial immune system for damage detection," in *Proceedings of the 7th European Workshop on Structural Health Monitoring (EWSHM '14)*, V. Le Cam, L. Melvel, and F. Schoefs, Eds., pp. 1341–1348, 2014.

[15] L. N. de Castro and J. Timmis, "Artificial immune systems: a novel approach to pattern recognition," in *Artificial Neural Networks in Pattern Recognition*, pp. 67–84, University of Paisley, 2002.

[16] A. K. Eroglu, Z. Erden, and A. Erden, "Bioinspired conceptual design (BICD) approach for hybrid Bioinspired robot design process," in *Proceedings of the IEEE International Conference on Mechatronics (ICM '11)*, pp. 905–910, April 2011.

[17] N. Cruz Cortés, *Sistema inmune artificial para solucionar problemas de optimización [Ph.D. thesis]*, Centro de Investigación y de Estudios Avanzados del Instituto Politécnico Nacional, 2004.

[18] P. J. Delves, S. J. Martin, D. R. Burton, and I. M. Roitt, *Roitt's Essential Immunology*, Wiley-Blackwell, 2011.

[19] L. N. de Castro and F. J. Von Zuben, "Artificial immune systems: part I basic theory and applications," Tech. Rep. DCA-RT 01/99, School of Computing and Electrical Engineering, State University of Campinas, Campinas, Brazil, 1999.

[20] D. T. Pérez, *Optimización global en espacios restringidos mediante un sistema inmune artificial [M.S. thesis]*, Centro de Investigación y de Estudios Avanzados del Instituto Politécnico Nacional, Mexico City, Mexico, 2005.

[21] U. Aickelin and D. Dasgupta, "Artificial immune system," in *Search Metodologies: Introductory Tutorials in Optimization and Decision Support Techniques*, pp. 375–399, Springer US, 2005.

[22] A. A. Freitas and J. Timmis, "Revisiting the foundations of artificial immune systems for data mining," *IEEE Transactions on Evolutionary Computation*, vol. 11, no. 4, pp. 521–540, 2007.

[23] R. Xiao and T. Chen, "Relationships of swarm intelligence and artificial immune system," *International Journal of Bio-Inspired Computation*, vol. 5, no. 1, pp. 35–51, 2013.

[24] X. Wang, X. Z. Gao, and S. J. Ovaska, "Fusion of clonal selection algorithm and harmony search method in optimisation of fuzzy classification systems," *International Journal of Bio-Inspired Computation*, vol. 1, no. 1-2, pp. 80–88, 2009.

[25] V. T. Nguyen, T. T. Nguyen, K. T. Mai, and T. D. Le, "A combination of negative selection algorithm and artificial immune network for virus detection," in *Future Data and Security Engineering: Proceedings of the 1st International Conference, FDSE 2014, Ho Chi Minh City, Vietnam, November 19–21, 2014*, vol. 8860 of *Lecture Notes in Computer Science*, pp. 97–106, Springer, Cham, Switzerland, 2014.

[26] N. Lay and I. Bate, "Applying artificial immune systems to real-time embedded systems," in *Proceedings of the IEEE Congress on Evolutionary Computation (CEC '07)*, pp. 3743–3750, IEEE, Singapore, September 2007.

[27] B. Mnassri, M. E. El Adel, and M. Ouladsine, "Fault localization using principal component analysis based on a new contribution to the squared prediction error," in *Proceedings of the 61th Mediterranean Conference on Control and Automation (MED '08)*, pp. 65–70, June 2008.

[28] A. Hyvarinen, J. Kahunen, and E. Oja, *Independent Component Analysis*, John Wiley & Sons, Hoboken, NJ, USA, 2001.

[29] D. A. Tibaduiza, L. E. Mujica, and J. Rodellar, "Damage classification in structural health monitoring using principal component analysis and self-organizing maps," *Structural Control and Health Monitoring*, vol. 20, no. 10, pp. 1303–1316, 2013.

[30] D. A. Tibaduiza, *Design and validation of a structural health monitoring system for aeronautical structures [Ph.D. thesis]*, Department of Applied Mathematics III, Universitat Politécnica de Catalunya, 2013.

[31] D. A. Tibaduiza, L. E. Mujica, A. Güemes, and J. Rodellar, "Active piezoelectric system using PCA," in *Proceedings of the 5th European Workshop on Structural Health Monitoring*, 2010.

[32] D.-A. Tibaduiza, M.-A. Torres-Arredondo, L. E. Mujica, J. Rodellar, and C.-P. Fritzen, "A study of two unsupervised data driven statistical methodologies for detecting and classifying damages in structural health monitoring," *Mechanical Systems and Signal Processing*, vol. 41, no. 1-2, pp. 467–484, 2013.

[33] J. A. Westerhuis, T. Kourti, and J. F. Macgregor, "Comparing alternative approaches for multivariate statistical analysis of batch process data," *Journal of Chemometrics*, vol. 13, no. 3-4, pp. 397–413, 1999.

[34] L. E. Mujica, M. Ruiz, F. Pozo, J. Rodellar, and A. Güemes, "A structural damage detection indicator based on principal component analysis and statistical hypothesis testing," *Smart Materials and Structures*, vol. 23, no. 2, Article ID 025014, 2014.

[35] D. A. Tibaduiza, L. E. Mujica, J. Rodellar, and A. Güemes, "Structural damage detection using principal component analysis and damage indices," *Journal of Intelligent Material Systems and Structures*, 2015.